Weld porosity in fibre laser weld of thixomolded heat resistant Mg alloys

L. Yu*[1], K. Nakata[1] and J. Liao[2]

Porosity in fibre laser welds of two thixomolded heat resistant magnesium alloys AE42 and AS41 was investigated in detail, and porosity formation mechanism was discussed in terms of gas compositions in porosity. It is found that the area percentage of porosity in welds decreases with increasing welding speed, and can be correlated to width of weld metal. Microstructure observation and gas composition analysis in porosity show that the porosity in welds is mainly attributed to the micropores pre-existing in base metals during melting of AE42 and AS41 alloys by fibre laser welding, which are formed due to air entrapment during thixomolding process. Hydrogen rejection and Ar shielding gas entrapment are also the possible reasons for the porosity formation; however, their contribution is much smaller than that of pores in base metals. Furthermore, the addition of rare earth element may probably decrease porosity amount in the thixomolded Mg alloys and their welds.

Keywords: Porosity, Fibre laser welding, Mg alloy, Gas inclusion, RE

Introduction

Under consideration of fuel economy in automotive and aerospace industries, Mg alloys have been adopted and are expected to be extensively used in the future, due to their lightweight and excellent specific mechanical properties.[1–3] At present, most of Mg alloy components in the automobiles are made by die-casting and thixomolding processes.[4] With the increasing demand of industrial application of Mg alloys, the development of welding technology for the assembling of Mg alloy parts becomes more and more important. Laser welding is one of potential assembling techniques to be widely employed in automobile industry; however, the study on laser welding of Mg alloy is still limited.[5–8] The objective of the authors' research is to investigate the fibre laser weldability of two thixomolded heat resistant Mg alloys AE42 and AS41.

Previous studies demonstrate that porosity in welds is one of the major concerns during laser welding of magnesium alloys, because it deteriorates mechanical properties, particularly tensile strength and elongation.[9] Until now, several mechanisms have been proposed to explain the formation of porosity in Mg alloys and their welds.[10–13] Mikuchi and Shearouse[10,11] have found that the amount of porosity in the solidified AZ91 alloy is proportional to the dissolved hydrogen in the alloy, and suggested that the rejection of hydrogen from the intermetallic compound $Mg_{17}Al_{12}$ assists in the nucleation and/or growth of micropores during the last stages of solidification. The difference in solubility between solid and liquid phases[12] indicates that hydrogen rejection from solid phase to liquid phase is a possible cause for porosity formation in the laser welds of Mg alloys. For AZ series forged alloys, Chi *et al.*[13] have reported that the pore formation in welds results from the dissolution of precipitates and recombination of oxygen atoms into molecules. Haferkamp *et al.*[14] have shown that there are more porosity in the fusion zone of non-vacuum die-cast AM60B alloy than that of vacuum die-cast AZ91D alloy, which implies that the presence of microporosity in the base metal (BM) is an important factor for the formation of porosity in Nd:YAG laser welds of Mg alloys. Through the detailed investigation of the porosity in the laser welds of die-cast AM60 alloy, Zhao and Debroy[15] and Pastor *et al.*[16] have concluded that microporosity preexisting in the BM is the origin of porosity in the laser welds, and proposed that the porosity in the welds is formed by the coalescing and expanding of micropores in the BM. They also suggested that remelting can remove some porosity in the welds. However, the porosity formation mechanisms proposed in the previous studies are based on only the observation of porosity in welds, without supporting from gas compositions analysis, which may lead to an incomplete conclusion. To comprehensively understand porosity formation mechanism in the weld of Mg alloys, both gas composition analysis in the porosity and porosity observation are necessary. In the present study, thixomolded Mg alloys AE42 and AS41 were welded with a high power fibre laser welding instrument, and the gas composition and volume in the porosity in the BMs and welds were measured using Quadruple-pole Mass Analysis Meter. On the basis of porosity observation and gas composition analysis in porosity, porosity formation mechanisms were discussed.

[1]Joining and Welding Research Institute, Osaka University, Osaka, Japan
[2]Kurimoto, Ltd, Osaka, Japan

*Corresponding author, email yuxueer33@hotmail.com

Published by Maney on behalf of the Institute
Received 4 February 2009; accepted 2 April 2009
DOI 10.1179/136217109X441209

Experimental

The materials used in the present study were heat resistant AE42 and AS41 Mg sheets, semisolid injection cast by thixomolding. The chemical compositions of the Mg alloys are listed in Table 1. The sheets were $150 \times 100 \times 5$ mm in specimen size, and the surface was degreased with acetone before welding. The samples were bead-on-plate welded by fibre laser welding system, under the conditions shown in Table 2. The laser power was fixed at 5 kW, while the welding speed was changed to be 2, 4, 6 and 10 m min^{-1}. Ar gas was used as shielding gas, and the flowrate of the shielding gas was 20 L min^{-1}.

After welding, metallographic inspections were performed on the cross-sections of the welded joints to examine the location and morphology of porosity in the welds and BMs. The specimens for metallographic inspections were first mechanically polished and then etched with different solutions: for AE42 alloy, the solution contained 1 mL nitric acid, 75 mL ethylene glycol and 24 mL water; for AS41 alloy, the solution consisted of 20 mL acetic acid, 60 mL ethylene glycol, 1 mL nitric acid and 20 mL water. The area percentage of porosity in the welds, i.e. the ratio of porosity area to weld cross-section area, was statistically measured using an image processing method (Image-Pro Plus ver.4·0). The average area percentage of porosity in three sections for each welding condition was used to evaluate the amount of porosity in the welds. The width of fusion zone (or weld metal, WM) was measured at three positions of fusion zone on each section, which are the top, the middle and the bottom, and the measurement was performed on three different sections for each welding condition. The average data of these measurements were used to represent the width of fusion zone in the present work.

In addition, the gas compositions in the porosity in welds and BMs were analysed using Anelva AGS-7000 Quadruple-pole Mass Analysis Meter, which can measure the gas released from the porosity by drilling the specimen in a vacuum chamber, with the parameters shown in Table 3. The diameter of the drill is 2 mm, and the depth of the drilled conical holes is $\sim$3 mm. More information on the analysis is described in Refs.17 and 18.

Table 1 Chemical compositions of thixomolded AE42 and AS41 Mg alloys

	Chemical compositions, mass-%					
Alloy	Al	Mn	Zn	RE*	Si	Mg
AE42	4·0	0·1	…	2·5	…	Bal.
AS41	4·2	0·20	…	…	1·0	Bal.

*RE refers to rare earth, primary Ce and a little Nd.

Table 2 Parameters of fibre laser welding

Laser power	5 kW
Welding speed	2–10 m min^{-1}
Shielding gas	100%Ar
Gas flowrate	20 L min^{-1}
Beam diameter	0·2 mm
Fibre diameter	0·1 mm
Focus length	250 mm
Forward incident angle	5°

Results and discussion

Porosity in fibre laser welds

Porosity on the cross-sections of the fibre laser welded joints of the two thixomolded Mg alloys at different welding speeds is shown in Fig. 1. The fusion boundary of the fibre laser welded joints is obvious; however, there is no distinct heat affected zone beside fusion zone, as reported by Liming *et al.*[19] There are large quantities of porosity in the welds of AE42 and AS41 alloys, irrespective of welding speeds. The pores in the fusion zones have various sizes from approximately 10 μm to 2 mm. The large pores are believed to be formed by the coalescence of small ones during welding. Some large pores are open to the surface of the specimens. The size of pores tends to decrease with increasing welding speed.

The relationship between the area percentage of porosity in WM and the welding speed is presented in Fig. 2, together with the width of WM at various welding speeds. It is evident that the area percentage of porosity in WM decreases with increasing welding speed for both the Mg alloys. This is accordant with the result in laser welding of die-cast AM60B alloy.[15,16] As compared with AS41 alloy, the area percentage of porosity in the WM of AE42 alloy is less. On the other hand, the width of WM also decreases monotonically with increasing welding speed, mainly because of the reduction of weld heat input per unit length of weld. The decrease in the area percentage of porosity in WMs with increasing welding speed is likely attributed to the reduction of the width of WM, since the porosity in WM come mainly from the micropores in the BMs, as described later. Besides, rare earth (RE)-containing AE42 alloy has a little narrower width of WM than AS41, probably due to their different melting points (e.g. 590 and 565 K for AE42 and AS41 respectively) as well as their different thermal diffusivities and fluidities. The narrower width of WM may contribute to the less area percentage of porosity in WMs of AE42 alloy.

Figure 3 reveals microstructure and pores at fusion boundary region in the weld of AE42 alloy at a welding speed of 10 m min^{-1}. It can be seen that pores exist in not only WM but also BM. The pores in WM are mainly regular spheres, whereas those in BM are quite irregular in morphology. It is likely to believe that the pores in WM come from those in BM by the coalescence of micropores in the BM in melting Mg alloys during welding. In order to confirm the origin of the porosity in the welds, however, gas composition analysis in the porosity is necessary.

Table 3 Parameters of Quadruple-pole Mass Analysis Meter for gas analysis

Ionisation energy	70 eV
CEM voltage*	−1400 V
Mass number range	2–100
Scanning time	0·52 s/scan
Beginning vacuum degree	About 5×10^{-6} Pa
Cutting-tool	2Φ drill

*CEM refers to channel electron multiplier.

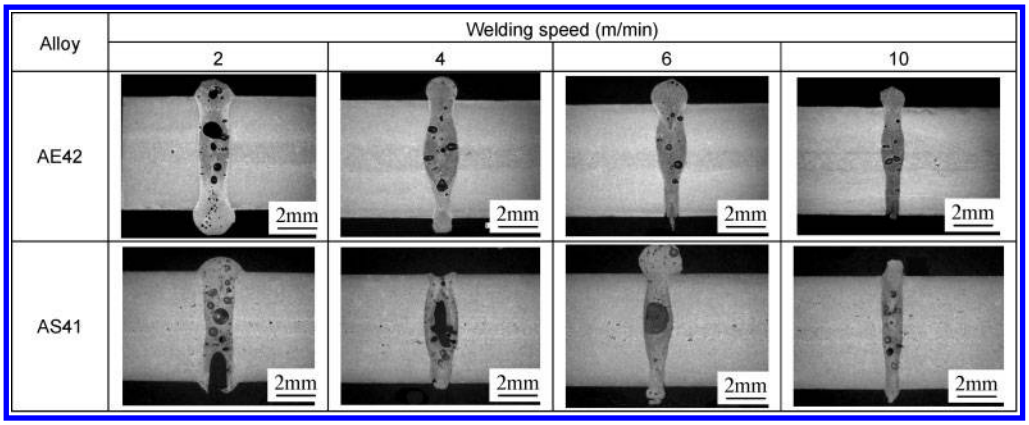

1 Macrostructures of cross-section of Mg alloy joints welded with 5 kW fibre laser power at different welding speeds

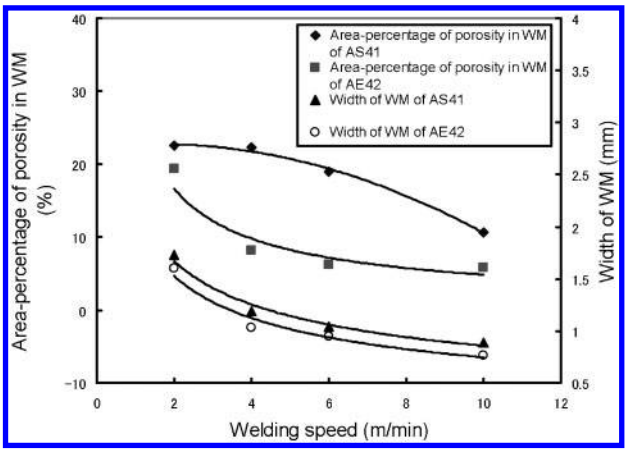

2 Relationship between area percentage of porosity in WM/width of WM and welding speed at constant laser power 5 kW

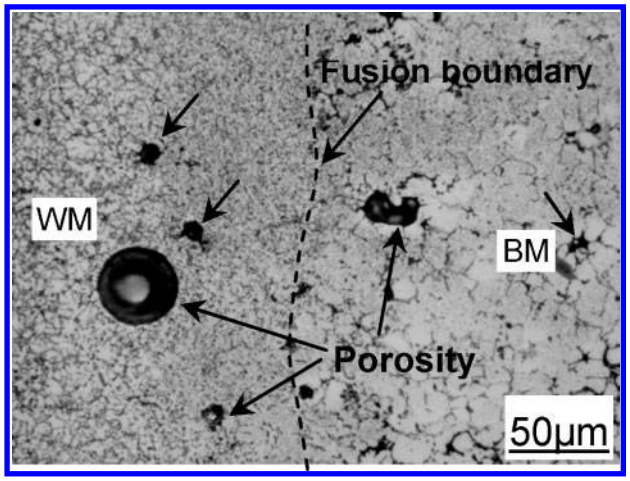

3 Porosity in both WM and BM of AE42 alloy welded at welding speed of 10 m min^{-1}

Gas compositions in porosity

The locations for gas compositions analysis in AE42 and AS41 alloys are illustrated in Fig. 4, showing the top-view of a sample and the drilled holes for gas analysis. Two points were analysed in BM and WM respectively for each Mg alloy. The specimens for gas composition analysis are those laser welded at a welding speed of 2 m min^{-1}.

The gas compositions and their volume at different positions are shown in Table 4. For AS41 alloy, it is obvious that N_2 is the major composition in porosity in both BM and WM; however, more H_2 is detected in WM than BM. For AE42 alloy, there is considerable H_2 in both BM and WM, apart from the major composition N_2. Like AS41 alloy, more H_2 exists in the porosity in WM than BM of AE42 alloy. In addition, some Ar is found in the porosity in WM of AE42 alloy. Regarding to the gas volume in AE42 and AS41alloys, it can be seen that the average gas volume in BM of AE42 is 2×10^{-4} mL, much less than the average gas volume $6{\cdot}5 \times 10^{-4}$ mL in BM of AS41 alloy. Less gas volume in BM of AE42 alloy is probably attributed to the presence of RE.

It's well known that N_2 is the main composition of air. From the morphology (Fig. 3) and gas compositions

Table 4 Gas composition and content of different positions in Mg alloy welds, %

Alloy	AS41				AE42			
Composition	WM ①	WM ②	BM ①	BM ②	WM ①	WM ②	BM ①	BM ②
H_2 (M/Z* 2)	4·8	3·1	0·4	0·4	30·5	10·2	14·1	1·7
CH_3 (M/Z 15)	0·1	0·1	<0·1	<0·1	1·7	1·0	1·8	2·0
H_2O (M/Z 18)	0·1	0·1	0·1	<0·1	0·5	<0·1	…	…
N_2 (M/Z 28)	94·3	96·0	98·8	98·9	65·2	81·1	82·3	94·6
C_xH_y (M/Z 29)	…	…	…	…	0·7	…	0·7	0·4
Ar (M/Z 40)	0·7	0·7	0·7	0·7	0·6	7·3	0·6	0·8
C_xH_y (M/Z 43)	<0·1	…	…	…	0·6	0·3	0·3	0·3
CO_2 (M/Z 44)	<0·1	<0·1	<0·1	<0·1	0·2	0·1	0·2	0·2
Total	100·0	100·0	100·0	100·0	100·0	100·0	100·0	100·0
Gas volume, mL	1×10^{-3}	1×10^{-3}	3×10^{-4}	1×10^{-3}	4×10^{-4}	2×10^{-4}	1×10^{-4}	3×10^{-4}

*M/Z refers to mass number.

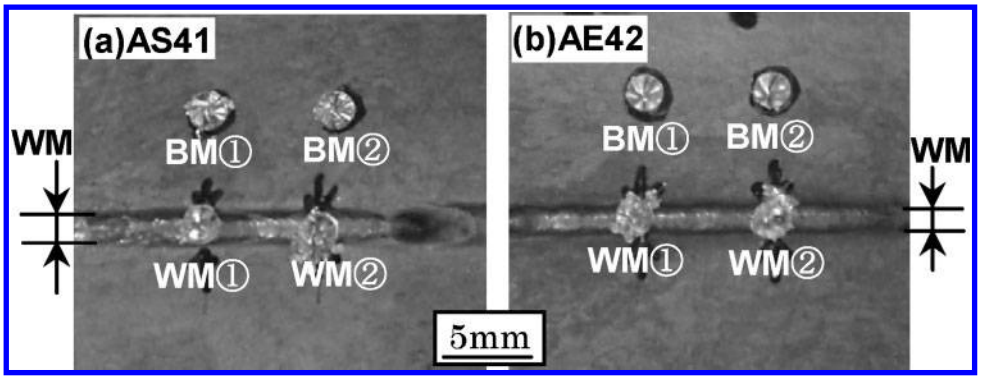

4 Gas analysis positions of Mg alloys in BM and WM

(Table 4) of pores in the BM, it can be believed that the pores in BMs of the thixomolded AE42 and AS41 alloys are mainly formed by air entrapment during thixomolding process. The O_2 in the air may be consumed by reacting with Mg to form magnesium oxides. Relatively high level of H_2 in the gas composition of the BM of thixomolded AE42 is probably due to the presence of 2·5 mass-% of RE element, which makes the alloy prone to hydrogen absorption.

Porosity formation mechanism in fibre laser weld of thixomolded Mg alloys

The porosity formation mechanisms in fibre laser welds of thixomolded Mg alloys are discussed as follows mainly on the basis of gas compositions analysis results in porosity.

It has been suggested that hydrogen in the BM is the main origin of porosity in the WM.[8,10,11] Because of the hydrogen solubility difference between the solid and liquid phases of Mg alloys, H_2 rejection from solid phase into liquid phase during solidification of welds is considered as the reason for porosity formation in the welds of Mg alloys. In the present study, the hydrogen content in the WMs is obviously higher than that in the BMs for both two Mg alloys. Therefore, H_2 rejection is a possible mechanism for the porosity formation in the welds.

However, N_2 is the principal composition in the porosity in welds for both two Mg alloys in the present study, and the N_2 content in the welds is almost equal to

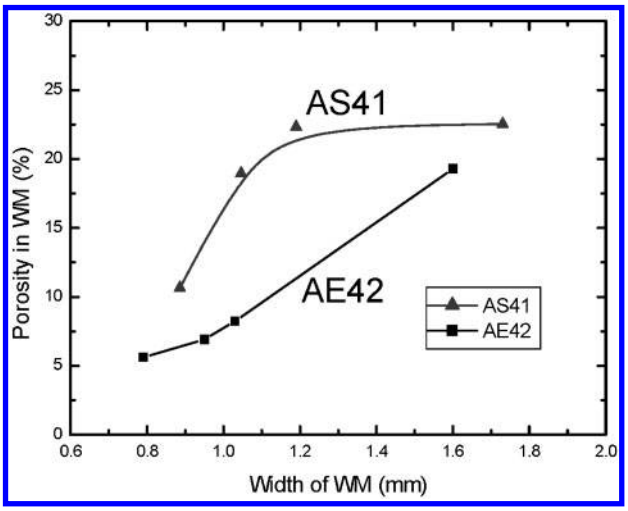

5 Relationship between porosity in WM and width of WM for AE42 and AS41 Mg alloys after welding

that in BMs. Hence, the porosity in the welds can be suggested to come mainly from the micropores in the BMs, which are formed mainly by air entrapment during thixomolding as mentioned previously. The present work supports the porosity formation mechanism proposed by Zhao and Debroy.[15,16] From the relationship between the area percentage of porosity in WM and the width of WM depicted in Fig. 5, it can be seen that the area percentage of porosity in WM increases with the increasing width of WM for each alloy. When the width of WM is larger, i.e. more BM is melted during welding, more micropores in BM are entrapped in WM, which leads to higher area percentage of porosity in WM. It can be suggested that the following steps are included in the formation process of porosity in welds. The first step is the gas release to molten WMs. In this step, gas in the micropores in BM is released into molten WM, as the BM is melted by laser energy during welding. The second is the expanding and coalescing of gas in the molten WMs. The gas in the molten WM expands because gas pressure in the molten WM is much lower than that in the solid BM, and the gas from neighbour pores coalesces. The third is the formation of large pores or blowholes in WMs. When the temperature of the molten WM lowers to below the melting point, the pores or blowholes with large size are formed in WMs. Because there is a three-dimensional expanding process, most porosity in WM reveals regular sphere in morphology.

It can also be seen that there is some Ar in the porosity in both BM and WM, and its content in WM of AE42 is higher than that in BM, as shown in Table 4. Small amount of Ar maybe comes from the air or oxidation preventing gas during thixo-molding process; however, the Ar content in WM of AE42 is 7·3 mass-%, much higher than that in the BM. This indicates that the Ar shielding gas is entrapped in WM during the welding process, due to the keyhole's instability, which is the dominant cause of porosity formation during laser welding of thin plates of Al alloys.[20] Therefore, the shielding gas entrapment during welding process is also a possible reason for the porosity formation in the WM.

In summary, three mechanisms are included in the porosity formation in fibre laser welds of thixomolded Mg alloys. The porosity in the welds is formed mainly by coalescence of micropores pre-existing in the BMs during melting BM by fibre laser welding. H_2 rejection and shielding gas entrapment also contribute to the porosity formation in the welds, but their contribution is not as tremendous as the micropores pre-existing in the

BM. In order to reduce the porosity in the welds, therefore, it is necessary to depress the formation of micropores in the BMs by preventing air entrapment during thixomolding process.

As described above, RE-containing AE42 alloy contains less porosity than AS41 alloy in BM. It is well known that RE is always added into Mg alloys to improve the creep resistance.[21] The present study shows that the addition of RE also tends to decrease the porosity amount in the Mg alloys. From a thermodynamic point of view, RE elements have a stronger affinity with the oxygen compared with that of Mg, so RE element can prohibit the reaction between Mg and oxygen during melting and casting process.[22] Therefore, RE can protect liquid and solid Mg from oxidation in a certain extent. In addition, RE increases the fluidity of Mg–Al alloys,[23] which results in notable decrease in casting defects including porosity. These may be the reasons that addition of RE element is beneficial to reduce the porosity in Mg alloys.

Conclusions

Based on the observation of porosity in the welds and gas composition analysis in porosity, the porosity formation mechanisms in fibre laser welds of thixomolded heat resistant AE42 and AS41 alloys were discussed. The major findings are as follows.

1. In fibre laser welds of the thixomolded Mg alloys, substantial weld porosity is formed in the WM. The area percentage of porosity in the welds decreases with increasing welding speed at a constant laser power. N_2 is the major composition in the porosity in both WMs and BMs of thixomolded Mg alloys.

2. Three mechanisms are included in the porosity formation in the fibre laser welds of the thixomolded Mg alloys. The porosity in the welds is mainly attributed to the micropores pre-existing in the BM, which are formed by air entrapment during thixomolding. Hydrogen rejection and Ar shielding gas entrapment during welding are also the possible mechanisms for the porosity formation in the welds of the Mg alloys; however, their contribution is much smaller, as compared to the micropores pre-existing in the BMs.

3. Less porosity is formed in RE-containing AE42 alloy than AS41 alloy. Addition of RE element seems to be beneficial to reduce the porosity in Mg alloy and their fibre laser welds.

References

1. X. Cao, M. Jahazi, J. P. Immarigeon and W. Wallace: *J. Mater. Process. Technol.*, 2006, **171**, 188–204.
2. N. Afrin, D. L. Chen, X. Cao and M. Jahazi: *Scr. Mater.*, 2007, **57**, 1004–1007.
3. B. L. Mordike, T. Ebert: *Mater. Sci. Eng. A*, 2001, **A302**, 37–45.
4. A. A. Luo, E. A. Nyberg, K. Sadayappan and W. Shi: *Magnesium Technol.*, 2008, 3–10.
5. A. Munitz, C. Cotler, A. Stern and G. Kohn: *Mater. Sci. Eng. A*, 2001, **A302**, 68–73.
6. G. M. Xie, Z. Y. Ma, L. Geng and R. S. Chen: *Mater. Sci. Eng. A*, 2007, **A471**, 63–68.
7. A. H. Feng and Z. Y. Ma: *Scr. Mater.*, 2007, **56**, 397–400.
8. J. H. Zhu, L. Li and Z. Liu: *Appl. Surf. Sci.*, 2005, **247**, 300–306.
9. L. Quintino, A. Costa, R. Miranda, D. Yapp, V. Kumar and C. J. Kong: *Mater. Design*, 2007, **28**, 1231–1237.
10. B. A. Mikucki and J. D. III Shearouse: Proc. Conf. on 'Magnesium properties and applications for automobiles', Detroit, MI, March 1993, Society of Automotive Engineers, Inc., 107–115.
11. J. D. III Shearouse and B. A. Mikucki: *J. Mater. Manuf.*, 1994, **103**, 542–552.
12. T. B. Massalski: 'Binary alloy phase diagrams', 2033–2036; 1986, Materials Park, OH, ASM International.
13. C. T. Chi, C. G. Chao, T. F. Liu and C. C. Wang: *Sci. Technol. Weld. Join.*, 2008, **13**, 199–211.
14. H. Haferkamp, F. W. Bach, I. Burmester, K. Kreutzburg and M. Niemeyer: Proc. 3rd Int. Conf. on 'Magnesium', (ed. G. W. Lorimer), 89–98; 1996, London, The Institute of Materials.
15. H. Zhao and T. Debroy: *Weld. J.*, 2001, **80**, 204s–210s.
16. M. Pastor, H. Zhao and T. Debroy: *J. Laser Appl.*, 2000, **12**, 91–100.
17. A. Ono, Y. Hayakawa, K. Ueki, J. Okayama and K. Ban: *Anal. Sci.*, 1994, **10**, 393–398.
18. T. Murakami, K. Nakata, T. Ikeda, H. Nakajima and M. Ushio: *Mater. Sci. Eng. A*, 2003, **A357**, 134–140.
19. L. Liming, W. Jifeng and S. Gang: *Mater. Sci. Eng. A*, 2004, **A381**, 129–133.
20. M. Pastor, H. Zhao, R. P. Martukanitz and T. Debroy: *Weld. J.*, 1999, **78**, 207s–216s.
21. S. M. Zhu, M. A. Gibson, J. F. Nie, M. A. Easton and T. B. Abbott: *Scr. Mater.*, 2008, **58**, 477–480.
22. X. K. Xi, R. J. Wang, D. Q. Zhao, M. X. Pan and W. H. Wang: *J. Non-Cryst. Solids*, 2004, **344**, 105–109.
23. Y. Lu, Q. Wang, X. Zeng, W. Ding, C. Zhai and Y. Zhu: *Mater. Sci. Eng. A*, 2000, **A278**, 66–76.